frontiers | Frontiers in Bioengineering and Biotechnology

ORIGINAL RESEARCH
published: 14 June 2022
doi: 10.3389/fbioe.2022.937489

An ICT-Based Coumarin Fluorescent Probe for the Detection of Hydrazine and Its Application in Environmental Water Samples and Organisms

Xina Liu[1†], Meiqing Zhu[2†], Chenyang Xu[1], Fugang Fan[1], Panpan Chen[1], Yi Wang[1] and Dongyang Li[3]**

[1]Anhui Provincial Key Laboratory of Quality and Safety of Agricultural Products, College of Resources and Environment, Anhui Agricultural University, Hefei, China, [2]School of Chemical and Environmental Engineering, Anhui Polytechnic University, Wuhu, China, [3]Laboratory of Agricultural Information Intelligent Sensing, College of Biosystems Engineering and Food Science, Zhejiang University, Hangzhou, China

OPEN ACCESS

Edited by:
Diming Zhang,
Zhejiang Lab, China

Reviewed by:
Yizhong Lu,
University of Jinan, China
Qing-Long Fu,
China University of Geosciences Wuhan, China

***Correspondence:**
Yi Wang
wangyi1987@cau.edu.cn
Dongyang Li
dylee@zju.edu.cn

†These authors have contributed equally to the work

Specialty section:
This article was submitted to Biosensors and Biomolecular Electronics, a section of the journal Frontiers in Bioengineering and Biotechnology

Received: *06 May 2022*
Accepted: *16 May 2022*
Published: *14 June 2022*

Citation:
Liu X, Zhu M, Xu C, Fan F, Chen P, Wang Y and Li D (2022) An ICT-Based Coumarin Fluorescent Probe for the Detection of Hydrazine and Its Application in Environmental Water Samples and Organisms. Front. Bioeng. Biotechnol. 10:937489. doi: 10.3389/fbioe.2022.937489

As an inorganic small molecule pollutant, the toxicity and potential carcinogenicity of hydrazine (N_2H_4) are of increasing concern. In this work, A water-soluble fluorescent probe (OCYB) based on the intramolecular charge transfer (ICT) mechanism for the detection of hydrazine was designed and synthesized. Taking the advantage of 4-bromobutyryl as the recognition group, the high selectivity of OCYB to N_2H_4 was confirmed by steady-state fluorescence spectroscopy. The limit of detection (LOD) was calculated to be 78 nM in the DMSO-HEPES (pH 7.4) system. The detection mechanism was verified by NMR, HRMS and density functional theory (DFT) calculations. In addition, OCYB exhibits strong anti-interference ability and an "Off-On" fluorescence enhancement effect. Importantly, OCYB can be used to effectively monitor the fluorescence distribution of N_2H_4 in environmental water samples and organisms.

Keywords: hydrazine, detection, density functional theory, imaging, fluorescent probe

INTRODUCTION

Hydrazine (N_2H_4) is a corrosive and highly reductive fine chemical raw material that is widely used in pharmaceuticals, chemistry, catalysis, agriculture, and other fields (Zhang et al., 2018; Wang et al., 2021). It is also used as a raw material for drugs, pesticides, dyes, foaming agents, contrast agents, antioxidants, and foaming agents (Zhang et al., 2020b). Despite its wide industrial applications, hydrazine is highly toxic and carcinogenic (Chen et al., 2021; Cui et al., 2022). Although not endogenous, trace spills during use or transportation can pollute the environment and enter the body by inhalation or skin contact, causing respiratory and neurological harm, including eye and skin irritation, liver, kidney, and central nervous system damage (Zhang et al., 2020a). At present, N_2H_4 has been classified as a carcinogen by the U.S. Environmental Protection Agency (EPA) with a threshold limit value (TLV) of 10 ppb (Xu W.-Z. et al., 2018; Yan et al., 2021). As the use of hydrazine increases, the risks become increasingly serious. The hazards of hydrazine are gradually being recognized and noticed. The development of a speedy, simple, sensitive, and selective method for detecting hydrazine is critical in the realm of environmental and biological sciences.

Many methods for the routine detection of hydrazine have been reported in recent years, such as titrimetric, spectrochemical, electrochemical, and surface-enhanced Raman spectroscopy, and chromatographic methods (Xu H. et al., 2018; Zhu et al., 2021b; Hu et al., 2021). Bo et al.

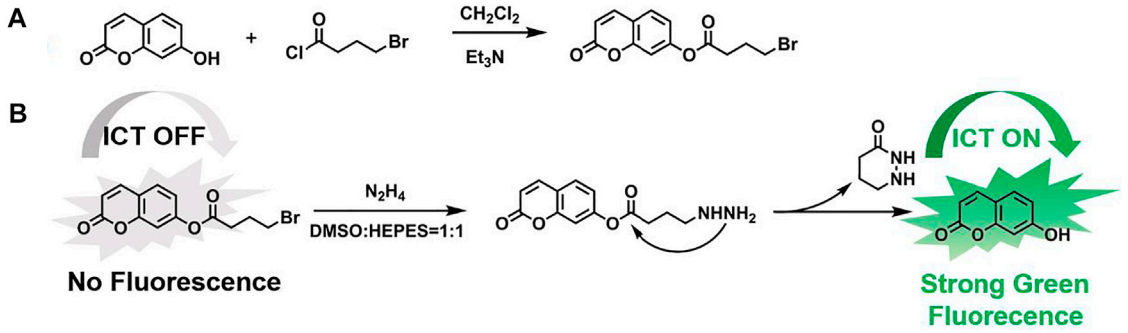

SCHEME 1 | (A) Synthetic route of OCYB and **(B)** Proposed mechanism for discriminative detection of N_2H_4.

developed a Pd/MCV composite electrode material for the electrochemical detection of hydrazine hydrate with a detection limit of 1.49×10^{-10} mol/L. Gu et al. used surface-enhanced Raman spectroscopy (SERS) to detect hydrazine in water with a detection limit of 8.5×10^{-11} mol/L (Gu and Camden, 2015). However, these assays have several drawbacks, such as the requirement for pretreatment of test samples, the preparation of reagents for testing, extended testing times, and sophisticated testing instruments (Guo et al., 2019; Qu et al., 2019). Furthermore, several of these assays have low sensitivity, are unable to detect low hydrazine concentrations, and cannot be utilized to detect hydrazine in biological samples (Chen et al., 2020; Jiang et al., 2020; Zhu et al., 2022). The advantages of fluorescence analysis include small sample size, great sensitivity, good reproducibility, speed, and convenience, among others (Yang et al., 2017; Zhu et al., 2019; Han et al., 2020; Yin et al., 2021). Fluorescence probe technology has advanced rapidly in both theory and application, and it is now widely employed in a variety of sectors including medicine, life science, and environmental science (Li et al., 2017; Yan et al., 2020; Cao et al., 2021). Many of these probes, however, still have issues including low selectivity, biocompatibility, and background interference, which severely limit their use in cells and *in vivo* (Na et al., 2016; Wang et al., 2017; Ye et al., 2021). Great structural modifiability, changeable excitation and emission wavelengths, high sensitivity, low cytotoxicity, and facile metabolic breakdown are all advantages of organic small-molecule fluorescent probes (Zhu et al., 2020; Zhu et al., 2021a; Ksenofontov et al., 2022). Therefore, it is significant to design and synthesize organic small-molecule fluorescent probes that are selective, sensitive, biocompatible, and capable of detecting hydrazine in cells and *in vivo*.

Coumarins are fluorophores with the parent ring structure of benzopyrone, and they are widely used as fluorophores for laser dyes, fluorescent brighteners, small-molecule fluorescent probes, and other applications because of their high fluorescence quantum yield, good light resistance, large Stokes shift, and adjustable optical properties. Coumarin does not glow by itself, but it can be changed with a variety of sites, such as inserting different types of groups at different places or linking multiple aromatic rings to increase the conjugation system, resulting in fluorescent dyes with a variety of emission bands. In the present study, a new recognition group was designed by the introduction of 7-hydroxycoumarin due to its excellent spectral performance and stability. 4-Bromobutyryl protected hydroxycoumarin to quench its fluorescence and improve the sensitivity and selectivity of the probe (Zhang et al., 2021). A 2-oxo-2H-chromium-7-yl 4-bromobutyrate (OCYB) is a relatively new probe designed and synthesized based on the intramolecular charge transfer (ICT) mechanism, which can detect N_2H_4 and exhibits specific recognition ability, strong anti-interference ability, and low detection limit. In addition, OCYB can also detect N_2H_4 in water samples and has been successfully applied to cell and zebrafish imaging.

EXPERIMENTAL SECTION

Reagents and Instruments

The experiments were carried out using an Agilent Cary Eclipse fluorescence spectrophotometer (Santa Clara, CA, United States) equipped with a xenon lamp and a quartz cuvette with a volume of 3.0 ml. The UV-Vis absorption spectra were performed on a Shimadzu UV-1900i spectrophotometer (Kyoto, Japan). pH values were obtained with a Shanghai Rex pH -25 digital display acidity meter (Shanghai, China). All nuclear magnetic resonance (NMR) spectra were recorded using an Agilent 600 MHz DD2 (DirectDrive2) spectrometer (Santa Clara, CA, United States). Analytical data for high-resolution mass spectrometry (HRMS) was collected with an Agilent Precision Mass Time of Flight Mass Spectrometer 6,520 mass spectrometer equipped with an electrospray ionization source. Hela cells and zebrafish imaging were investigated with an EVOS fluorescence auto-inverted fluorescence microscope (Waltham, MA, United States) and a Nikon inverted fluorescence microscope (Tokyo, Japan), respectively.

N_2H_4, 4-bromobutyryl chloride and triethylamine were purchased from Bailingwei Technology Co. Ltd (Beijing, China), Ciensi Biochemical Technology Co., Ltd. (Tianjin, China) and Aladdin Reagent Co., Ltd (Shanghai, China). Tryptophan (Try), tyrosine (Tyr), arginine (Arg), histidine (His), lysine (Lys), aspartic acid (Asp), threonine (Thr), glutamic acid (Glu) and glycine (Gly) were obtained from Sinopharm Chemical Reagent Co., Ltd (Shanghai, China).

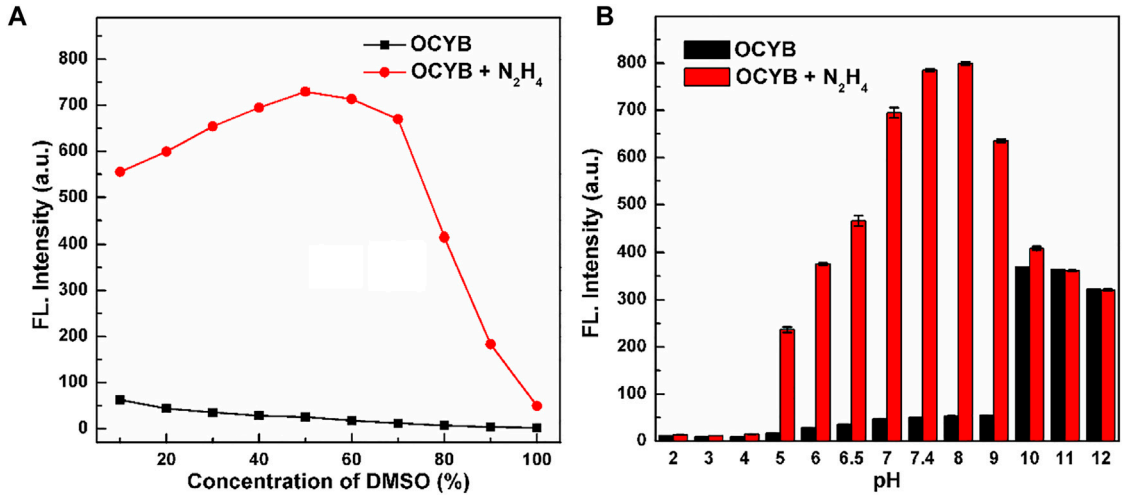

FIGURE 1 | Ratiometric response ($I_{458\ nm}/I_{330\ nm}$) of OCYB (10 μM) without and with N_2H_4 (200 μM) in HEPES buffer solution containing **(A)** 10–100% DMSO and **(B)** at different pH with DMSO = 50%. Data are shown as the mean ± SE (bars) (n = 3).

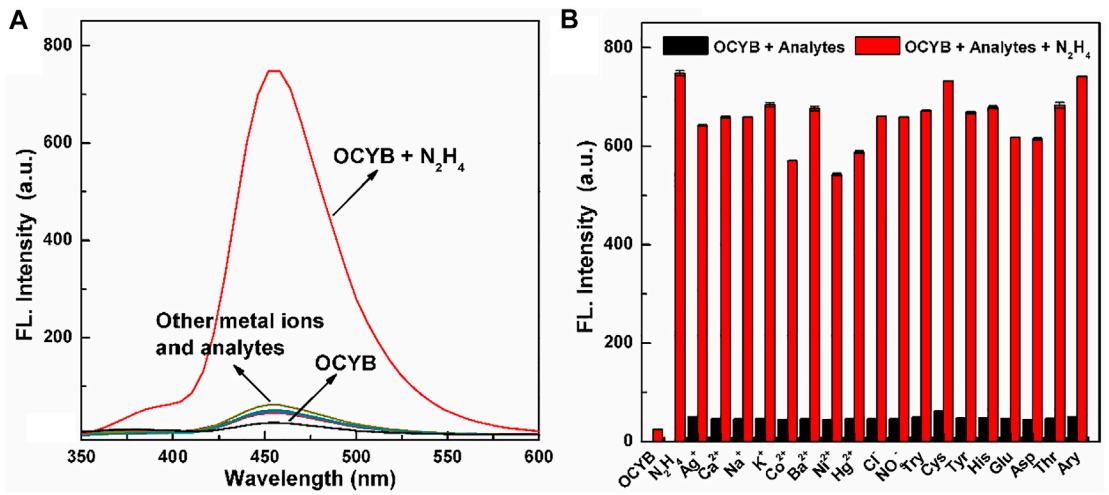

FIGURE 2 | Fluorescence spectra **(A)** of OCYB (10 μM) in the presence of different interference analytes. **(B)** The fluorescence intensity of OCYB and N_2H_4 (200 μM) in the presence of other interference analytes (200 μM) in DMSO-HEPES buffer solution (1:1, v/v, pH 7.4, λ_{ex} = 330 nm). Data are shown as the means ± SE (bars) (n = 3).

Other reagents were all obtained from Xilong Chemical Co., Ltd. (Guangdong, China). All chemical reagents are directly used in the experiment without further purification. Deionized water (18.25 MΩ cm) from the Milli-Q® Direct 8 & 16 Ultrapure Water System (Billerica, MA, United States) was used to prepare the aqueous solution for the experiment. All glass containers are rinsed three times with deionized water before use.

Synthesis and Characterization of OCYB

The coumarin-like fluorescent probe OCYB was produced using a theoretically derived approach (**Scheme 1A**). 7-Hydroxycoumarin (2.0 g, 12.3 mmol) and triethylamine (1.87 g, 18.5 mmol) were mixed in CH_2Cl_2 and cooled to 0 °C. Then, 4-bromobutyryl chloride (2.73 g, 14.8 mmol) was slowly added to the solution using a constant pressure dropper and the mixture was stirred at room temperature for 3 h. After the concentration under reduced pressure, the crude product was purified by chromatography into 2-oxo-2H-chromium-7-yl 4-bromobutyrate and the probe OCYB was obtained (3.2 g, 83.6%). ^{13}C NMR (151 MHz, DMSO-d_6) δ 170.96, 160.08, 154.53, 153.24, 144.23, 129.72, 119.01, 115.99, 110.46, 34.21, 32.65, 28.09, 27.91. ^{1}HNMR (600 MHz, DMSO-d_6) δ 8.05 (d, J = 9.6 Hz, 1H), 7.75 (d, J = 8.4 Hz, 1H), 7.28 (d, J = 2.2 Hz, 1H), 7.16 (dd, J = 8.4, 2.2 Hz, 1H), 6.45 (d, J = 9.6 Hz, 1H), 3.62 (t, J = 6.6 Hz, 2H), 2.76 (t, J = 7.3 Hz, 2H), 2.19 – 2.15 (m, 2H).

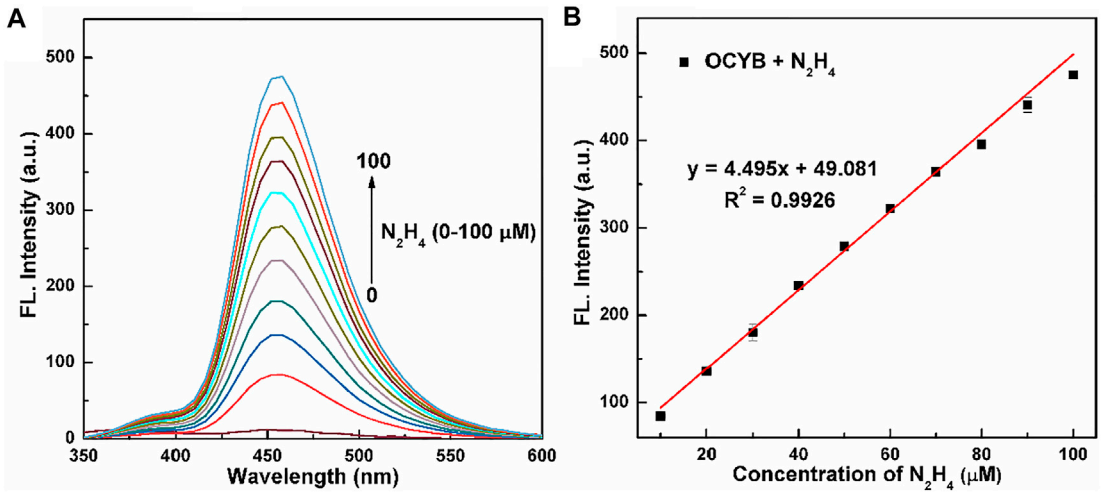

FIGURE 3 | Fluorescence spectra **(A)** of OCYB (10 μM) with a series of concentrations of N_2H_4 (0–100 μM) in DMSO-HEPES buffer solution (1:1, v/v, pH 7.4, λ_{ex} = 330 nm). The linear relationship between the fluorescence intensity **(B)** of OCYB and the N_2H_4 concentration (0–100 μM). Data are shown as the mean ± SE (bars) (n = 3).

Optical Properties of OCYB

Spectroscopic analysis was performed in a mixture of DMSO and 2-[4-(2-hydroxyethyl)-1-piperazinyl] ethanesulfonic acid HEPES (1:1, v/v, pH = 7.4). The probe OCYB was dissolved in DMSO and made into a 10 mM stock solution; the analytes $AgNO_3$, $Ca(NO_3)_2$, $NaNO_3$, KNO_3, NaCl, $CoCl_2$, $BaCl_2$, $NiCl_2$, $HgCl_2$, and amino acids Try, Cys, Tyr, His, Glu, Asp, Thr, Ary were configured into a 5×10^{-3} M solution. After the addition of the analytes, the spectra of UV-vis and fluorescence were recorded using a 3 ml volume quartz cuvette. The conditions were set as follows: E_x = 330 nm, E_m = 350–700 nm.

Cell Culture and Cellular Imaging

HeLa cells were cultured in 96-well plates for 24 h at 37°C. A series of probe solutions (10, 20, 30 and 40 μM) in a concentration gradient was added to 96-well culture plates containing HeLa cells (5×10^{-4} cells per well incubated), and untreated HeLa cells were used as controls. After 24 h of incubation, the cell viability of HeLa cells was determined by the CCK-8 assay.

Untreated HeLa cells were used as control. The wells of the plate containing Hela cells were incubated for 24 h and then treated for 30 min with N_2H_4 solution (50 μM). Then, HeLa cells were treated with OCYB (20 μM) for 20 min in a constant temperature incubator and washed three times with PBS solution to remove the excess N_2H_4. Finally, untreated HeLa cells and treated HeLa cells were imaged using an Eclipse TiS fluorescence microscope (Nikon, Japan).

Imaging of Zebrafish

Zebrafish eggs were incubated in an E3 medium containing nutrient salts (sodium bicarbonate, $CaCl_2 \bullet 2H_2O$, $MgSO_4 \bullet 7H_2O$ and KCl) and placed at a constant temperature incubator at 28°C. Normally growing 3d zebrafish were selected for the experiment. The zebrafish were first incubated in the E3 medium with N_2H_4 solution (final concentration of 100 μM) for 30 min and then treated with OCYB (20 μM) for 30 min. Zebrafish without N_2H_4 was used as blank control. Zebrafish were anesthetized with tricaine (50 mg/L) during the experiment and imaged using an Olympus BX41-32P02-FLB3 fluorescence microscope (Tokyo, Japan).

Treatment of Water Samples

Water samples for this experiment were collected from rivers around parks and schools in the Hefei area of Anhui, China, as test water samples. The same concentration of HEPES buffer was prepared separately with different water samples. Then N_2H_4 was added at 0.1, 0.5, and 1 mg/L. The OCYB probe solution was incubated with the samples for 1 h, and the fluorescence spectra of each sample were recorded (E_x = 330 nm). The intercept of the standard addition curve was used to calculate the concentration of N_2H_4 in the raw water samples.

RESULTS AND DISCUSSION

Structural Characterization of OCYB

Because of its excellent spectroscopic properties and stable absorption, OCYB was designed and synthesized using the intramolecular charge transfer (ICT) mechanism by introducing the 4-bromobutyryl group as a recognition group in 7-hydroxycoumarin, and the synthetic route for high-yield OCYB is shown in **Scheme 1A**. The possible recognition mechanism of probe OCYB to N_2H_4 is shown in **Scheme 1B**. The ICT process is disturbed and the probe OCYB is not fluorescent because the hydroxyl group in the probe OCYB is shielded by 4-bromobutyryl. When N_2H_4 is introduced to the probe OCYB, it works as a nucleophilic reagent, attacking the 4-bromobutyryl group and undergoing a substitution-cyclization reaction, resulting in a "turn-on" phenomenon and green fluorescence. The apparent change in fluorescence intensity before and after the interaction of the probe OCYB with N_2H_4 was used to specifically identify and detect N_2H_4. This was

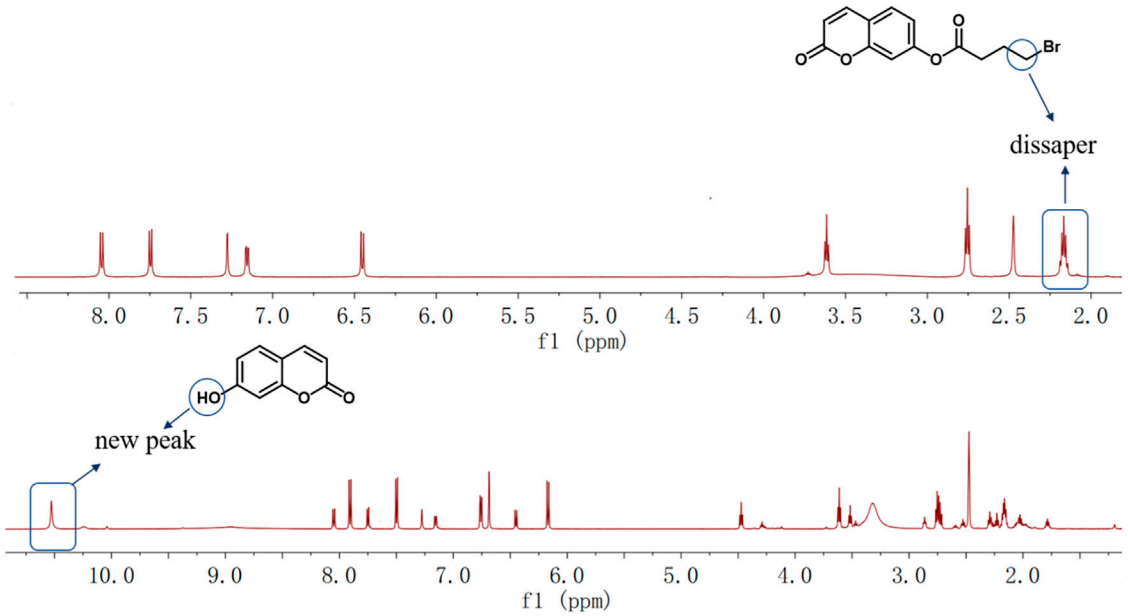

FIGURE 4 | ^{1}H NMR spectra of OCYB before and after adding N_2H_4.

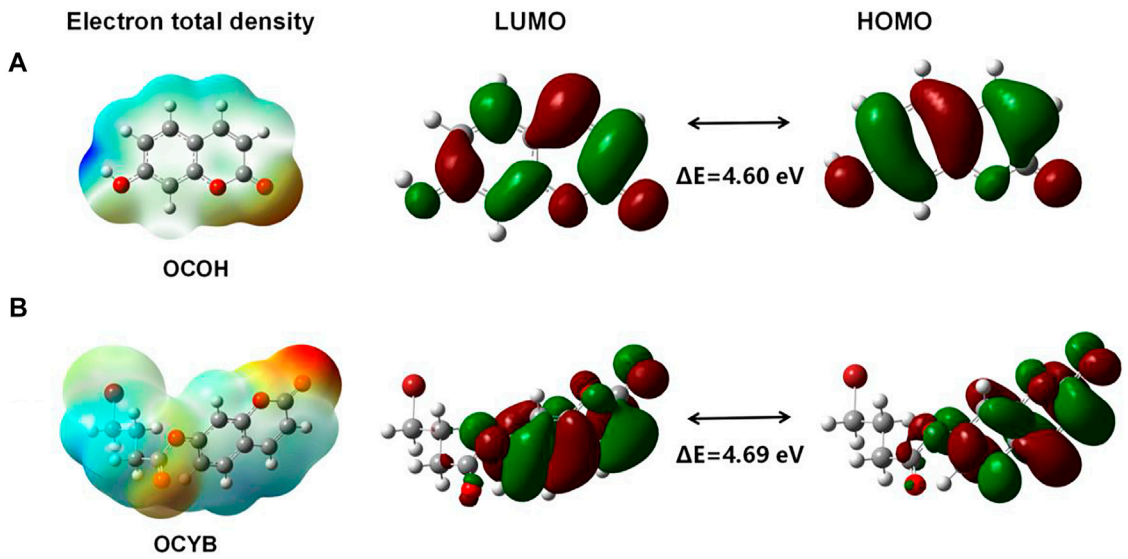

FIGURE 5 | Quantum chemical calculations of OCOH **(A)** and OCYB **(B)**.

confirmed by ^{1}H NMR, ^{13}C NMR and HRMS (**Supplementary Figure S1-3**).

Optimization of Reaction Conditions

The reaction conditions between the probe OCYB and N_2H_4 were optimized to obtain the best experimental conditions. The highest fluorescence intensity of the OCYB-N_2H_4 system was established by testing different DMSO concentrations, resulting in the discovery of the best-matched solvent ratio for the reaction between OCYB and N_2H_4 (**Figure 1A**). The influence of pH on the detection system was also studied. As shown in **Figure 1B**, the probe showed essentially no change in fluorescence intensity (I_{458nm}) at pH 2-9, while the OCYB-N_2H_4 system showed a significant emission signal in the pH 7-9 range following reaction with N_2H_4 (200 μM). Considering the application of OCYB *in vivo* and *in vitro*, we chose pH 7.4 according to its physiological conditions. Based on the above reaction conditions, we further studied the effect of the reaction time between OCYB

TABLE 1 | Determination of N_2H_4 in real water samples.

Samples	Concentration of N_2H_4		Recovery (%)
	Added Amount (mg/L)	Recovered Amount (mg/L)	
Pure Water (Hefei, Anhui)	0.10	0.09 ± 0.01	90
	0.50	0.52 ± 0.01	104
	1.00	1.02 ± 0.02	102
Blackpool Dam Water (Hefei, Anhui)	0.10	0.09 ± 0.01	90
	0.50	0.47 ± 0.03	94
	1.00	0.99 ± 0.01	99
Moat water (Hefei, Anhui)	0.10	0.10 ± 0.02	100
	0.50	0.46 ± 0.01	92
	1.00	0.93 ± 0.04	93
Pond Water (Anhui Agricultural University)	0.10	0.08 ± 0.02	80
	0.50	0.48 ± 0.01	96
	1.00	0.97 ± 0.02	97

[a]*The above water sample is taken at multiple points, and the sampling point is not less than 5. Data are mean ± SE (bars) (n = 3).*

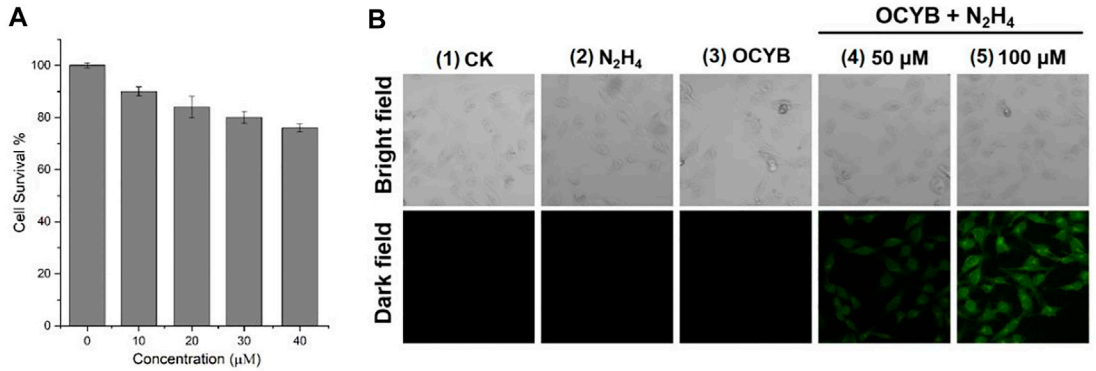

FIGURE 6 | (A) Cell survival of different concentration of OCYB; **(B)** Fluorescence images for HeLa cells (1: blank control. 2: N_2H_4. 3: OCYB. 4 and 5: HeLa cells were treated with OCYB and then incubated with N_2H_4, Ex = 375 nm).

and N_2H_4. The fluorescence ratio response of the reaction system rose as the reaction time grew after adding N_2H_4 to the OCYB probe solution. Because the system remained stable after 1.5 h, the reaction time was fixed to 1.5 h in the following trials (**Supplementary Figure S4**).

Selectivity and Anti-interference of OCYB Against N_2H_4

We did additional research after determining that the OCYB probe can react with N_2H_4 using the preceding experiments and identifying the reaction's ideal parameters. To determine whether the OCYB probe can specifically recognize N_2H_4, we selected a series of ions (Ag^+, Ca^{2+}, Na^+, K^+, Co^{2+}, Ba^{2+}, Ni^{2+}, Hg^{2+}, NO_3^-, Cl^-) and compounds (Try, Cys, Tyr, His, Glu, Asp, Thr, Ary) to study the effect on the DDPB probe. With the addition of ions and various analytes, the fluorescence characteristics of the OCYB-N_2H_4 probe did not change. But when N_2H_4 was added, the fluorescence spectrum of the OCYB-N_2H_4 system was significantly enhanced (**Figure 2A**). Only the fluorescence intensity of the OCYB-N_2H_4 combination is dominating at an excitation wavelength of 330 nm, whereas other investigations only reveal the smallest fluorescence response in the presence of OCYB. The preceding data show that the OCYB probe detects N_2H_4 with good selectivity.

Subsequently, the anti-interference ability of the OCYB probe was continued. The fluorescence intensity of the OCYB probe changed significantly with the addition of N_2H_4 and the coexistence of anions, cations and typical bioanalytics did not effect on the detection of N_2H_4 by probe OCYB (**Figure 2B**). Thus, the OCYB probe has good specificity and strong resistance to interference for the detection of N_2H_4 and can be used in complex systems or environments.

Response of OCYB to N_2H_4

The sensitivity and linear range of the probe OCYB were further investigated using N_2H_4 fluorescence titration experiments, as shown in **Figure 3a**, which recorded the variation of the probe OCYB (10 μM) fluorescence emission spectrum in DMSO-HEPES buffer (1:1, v/v, pH 7.4) in the range of 0–100 μM of N_2H_4 concentration. The probe OCYB did not fluoresce on its own, but the fluorescence intensity at 458 nm grew dramatically

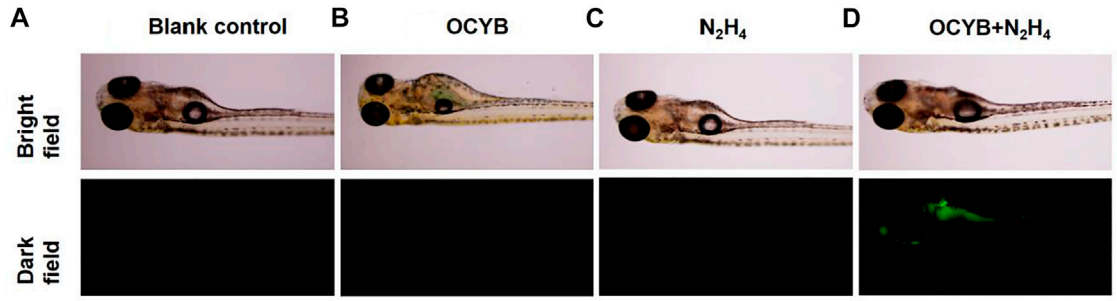

FIGURE 7 | Fluorescence images of zebrafish: **(A)** blank control. **(B)** OCYB. **(C)** zebrafish incubated with N_2H_4 (100 μM) for 30 min **(D)** zebrafifish samples pretreated with N_2H_4 (100 μM) for 30 min before incubation with OCYB (20 μM) for 30 min (Ex = 375 nm).

as the N_2H_4 concentration was increased. In the concentration range of 0–100 μM, there is a good linear relationship between the fluorescence intensity y of the probe OCYB and the concentration x of N_2H_4, as shown in **Figure 3B**, with the regression equation y = 4.4951x + 49.0814 (R^2 = 0.9926), indicating that the probe OCYB can quantitatively detect N_2H_4 over a wide range. According to the equation LOD = 3N/S (LOD, N, and S are the detection limit, noise (mV), and slope, respectively), the LOD of the OCYB probe was calculated to be 78 nM, which is much lower than the US EPA's threshold limit (0.31 μM), indicating that the probe OCYB has a good detection sensitivity for N_2H_4.

Reaction Mechanism

Bromoester derivatives are known to react with N_2H_4 by nucleophilic substitution of bromine groups and nucleophilic addition of ester carbon groups, followed by intramolecular cyclization to release fluorophores. For understanding the reaction mechanism of the probe OCYB on N_2H_4, we compared the ^{1}H NMR spectra of OCYB and OCYB-N_2H_4 system (**Figure 4**). The hydrogen peak near the bromine atom on the 4-bromobutyryl group arises at 2.0–2.4 ppm, as illustrated in the image. The hydrogen peak near the bromine atom vanishes once the reaction of OCYB with N_2H_4 is completed, and a new peak at 10.5 ppm appears. These results suggest that OCYB undergoes a substitution-cyclization reaction triggered by N_2H_4 that releases fluorescent groups, which enhances the fluorescence signal. To corroborate the aforesaid mechanism, we used HRMS to investigate the OCYB-N_2H_4 product (**Supplementary Figure S5**) and found a signal at m/z=163.0386, which is nearly identical to the theoretical molecular weight of 7-hydroxycoumarin ($[M+H]^+$ = 163.0317). The above findings suggest that OCYB experienced a substitution process triggered by N_2H_4, resulting in the release of the 7-hydroxycoumarin fluorophore and a shift in the fluorescence signal (**Scheme 1B**).

Computational Study of OCYB

The molecular structure and charge distribution of OCYB and its product OCOH were simulated using density general function theory (DFT) calculations (B3LYP/6–31*G) to gain insight into the sensing mechanism of OCYB on N_2H_4. The optimized molecular structures of OCOH and OCYB are shown in **Supplementary Figures S6, S7**. The fluorescence enhancement of OCYB induced by N_2H_4 is mainly summarized in two aspects. The phenolic hydroxyl group on OCYB belongs to the electron-absorbing group (acceptor) and the 4-bromobutyryl group as the electron-donating group (donor) forms a π-π conjugation system. The intramolecular transfer of electrons from the donor to the acceptor enhances the fluorescence, while the modification of the hydroxyl group on OCOH by the 4-bromobutyryl group blocks this process, resulting in a fluorescence quenching (**Figure 5**). The donor in the fluorophore reacts with the target molecule with an enhanced electron absorption capacity of the acceptor and a change in the LUMO/HOMO energy level difference of the fluorophore (4.69–4.60 eV). The reaction of OCYB and N_2H_4 was also shown to be based on an intramolecular charge transfer (ICT) mechanism, which results in increased fluorescence of the probe OCYB.

Practical Applications

Water samples were gathered from rivers near parks and schools in Hefei, Anhui, China, as test water samples for the assessment and analysis of N_2H_4 using OCYB to evaluate the probe's practical application in detecting N_2H_4. The OCYB probe was introduced to a water sample having a 10 μM N_2H_4 gradient concentration. The fluorescence spectra of OCYB-N_2H_4 in water samples were recorded, and a standard addition curve was created using the specific fluorescence intensity as the y-axis and the amount of N_2H_4 supplied as the x-axis (**Supplementary Figure S8**). According to **Table 1**, N_2H_4 detection fluorescence recoveries ranged from 80 to 104%, showing that the probe OCYB was successful in detecting N_2H_4 in actual solutions.

Cellular Experiments

The survival rate of HeLa cells treated with MTT colorimetric assay at varying doses of OCYB solution for 24 h was used to determine the survivability of the probe OCYB for *in vivo* research. The survival rate of HeLa cells in all four groups decreased with increasing probe concentration (**Figure 6A**). The greatest concentration of OCYB used was 40 μM, and HeLa cells survived 76% of the time at this concentration, with the average survival rate of the four groups being 83%. The results of the foregoing experiments show that the probe OCYB has low cytotoxicity and can be employed *in vivo* studies.

N_2H_4 in the environment, ingested by creatures through the mouth, nose, or skin surface, has powerful toxic effects on species, and if ingested by humans, can cause serious harm to the human system. Therefore, the study of fluorescence imaging of N_2H_4 in living cells is an important guideline for both biological research and the development of the pharmaceutical industry. HeLa cells were used to test the fluorescence imaging ability of OCYB in living cells in this study (**Figure 6B**). No fluorescence was recorded in HeLa cells from blank control, only OCYB, and containing N_2H_4 under the fluorescence channel. Correspondingly, after treatment with OCYB and then incubation with N_2H_4 (50 μM, 100 μM), the distribution of strong green fluorescence in HeLa cells could be seen under fluorescence. It can also be seen that the fluorescence intensity of the group 5 at N_2H_4 (100 μM) is higher, and the image is clearer. This is due to the release of more fluorescent groups due to the reaction of OCYB with the added exogenous N_2H_4. The intracellular fluorescence changes caused by N_2H_4 imply that OCYB penetrates HeLa cells well and is responsive to extracellular and extracellular sources of N_2H_4, allowing N_2H_4 imaging in living HeLa cells.

Zebrafish Imaging

Because zebrafish and human genes have an 87% genetic similarity, zebrafish were chosen as the subject for *in vivo* fluorescence imaging of hydrazine. As shown in **Figure 7**, there was no significant differential change in zebrafish between the four treatment conditions under bright field conditions. However, zebrafish incubated with N_2H_4 (100 μM) under darkfield conditions and then treated with OCYB for 30 min showed a strong bright green fluorescence effect. The green fluorescence is mainly found in the head, stomach, respiratory tract and digestive tract of zebrafish. The experimental results showed that the fluorescent probe OCYB could enter zebrafish and visualize the distribution of N_2H_4 in the organism. It is also further demonstrated that OCYB presents low toxicity with little biological hazard.

CONCLUSION

In conclusion, a coumarin-based hydrazine-specific detection fluorescent probe OCYB based on the ICT mechanism was synthesized in this paper. The key features of OCYB include easy availability of raw materials, low cost, large Stokes shift (128 nm), low detection limit (78 nM), low toxicity, good cell permeability, and high selectivity. HRMS, NMR, and DFT calculations were used to verify the mechanism of the reaction between OCYB and N_2H_4. According to the results of the practical application, OCYB can be used to detect N_2H_4 in real water samples. Furthermore, due to its low cytotoxicity and good biocompatibility, OCYB has also been successfully applied for imaging endogenous N_2H_4 in live HeLa cells and zebrafish. The present study provides important information for the visual detection of environmental contaminants.

DATA AVAILABILITY STATEMENT

The original contributions presented in the study are included in the article/**Supplementary Material**, further inquiries can be directed to the corresponding authors.

AUTHOR CONTRIBUTIONS

XL: Conceptualization, Formal analysis, Investigation, Data curation, Writing—original draft, Writing—review and editing, Visualization. MZ: Methodology, Formal analysis, Validation, Data curation. FF: Methodology, Formal analysis, Validation, Data curation. CX: Data curation, Writing—original draft, Writing—review and editing, Visualization. PC: Resources, Data curation, Writing—review and editing. YW: Methodology, Formal analysis, Validation, Data curation. DL: Supervision, Data curation, Writing—review and editing.

FUNDING

The authors gratefully acknowledge financial support from the National Natural Science Foundation of China (No. 32072464), the Elite Project of Shennong Scholar of Anhui Agricultural University and the Scientific Research Start-up Fund for Introduced Talents of Anhui Polytechnic University (No. 2021YQQ052).

SUPPLEMENTARY MATERIAL

The Supplementary Material for this article can be found online at: https://www.frontiersin.org/articles/10.3389/fbioe.2022.937489/full#supplementary-material

REFERENCES

Cao, X. L., Bai, Y. G., Li, F., Liu, F. X., and Yu, X. Y. (2021). A Facile Synthesis of Tannic Acid-Protected Copper Nanoclusters and the Sensitive Fluorescence Detection of Nitrite Ion under Mild Conditions. *Spectroscopy* 36 (5), 22–27. doi:10.1002/bio.3942

Chen, C., Zhao, D., Wang, B., Ni, P., Jiang, Y., Zhang, C., et al. (2020). Alkaline Phosphatase-Triggered *In Situ* Formation of Silicon-Containing Nanoparticles for a Fluorometric and Colorimetric Dual-Channel Immunoassay. *Anal. Chem.* 92 (6), 4639–4646. doi:10.1021/acs.analchem.0c00224

Chen, R., Shi, G.-J., Wang, J.-J., Qin, H.-F., Zhang, Q., Chen, S., et al. (2021). A Highly-Sensitive "turn on" Probe Based on Coumarin β-diketone for Hydrazine Detection in PBS and Living Cells. *Spectrochimica Acta Part A Mol. Biomol. Spectrosc.* 252, 119510. doi:10.1016/j.saa.2021.119510

Cui, Y., Xu, C., Wu, T., Nie, Y., and Zhou, Y. (2022). Near-infrared Cyanine-Based Fluorescent Probe: Rapidly Visualizing the *In Situ* Release of Hydrazine in Living Cells and Zebrafish. *Sensors Actuators B Chem.* 350, 130878. doi:10.1016/j.snb.2021.130878

Gu, X., and Camden, J. P. (2015). Surface-Enhanced Raman Spectroscopy-Based Approach for Ultrasensitive and Selective Detection of Hydrazine. *Anal. Chem.* 87 (13), 6460–6464. doi:10.1021/acs.analchem.5b01566

Guo, S.-H., Guo, Z.-Q., Wang, C.-Y., Shen, Y., and Zhu, W.-H. (2019). An Ultrasensitive Fluorescent Probe for Hydrazine Detection and its Application in Water Samples and Living Cells. *Tetrahedron* 75 (18), 2642–2646. doi:10.1016/j.tet.2019.03.022

Han, J., Yue, X., Wang, J., Zhang, Y., Wang, B., and Song, X. (2020). A Ratiometric Merocyanine-Based Fluorescent Probe for Detecting Hydrazine in Living Cells and Zebra Fish. *Chin. Chem. Lett.* 31 (6), 1508–1510. doi:10.1016/j.cclet.2020.01.029

Hu, S., Wang, J., Luo, M., Wu, Z., Hou, Y., and Chen, X. (2021). A Novel ESIPT Fluorescent Probe Derived from 3-hydroxyphthalimide for Hydrazine Detection in Aqueous Solution and Living Cells. *Anal. Bioanal. Chem.* 413 (21), 5463–5468. doi:10.1007/s00216-021-03530-1

Jiang, X., Lu, Z., Shangguan, M., Yi, S., Zeng, X., Zhang, Y., et al. (2020). A Fluorescence "Turn-On" Sensor for Detecting Hydrazine in Environment. *Microchem. J.* 152, 104376. doi:10.1016/j.microc.2019.104376

Ksenofontov, A. A., Bocharov, P. S., Ksenofontova, K. V., and Antina, E. V. (2022). Water-Soluble BODIPY-Based Fluorescent Probe for BSA and HSA Detection. *J. Mol. Liq.* 345, 117031. doi:10.1016/j.molliq.2021.117031

Li, B., He, Z., Zhou, H., Zhang, H., Li, W., Cheng, T., et al. (2017). Reaction Based Colorimetric and Fluorescence Probes for Selective Detection of Hydrazine. *Dyes Pigments* 146, 300–304. doi:10.1016/j.dyepig.2017.07.023

Na, R., Zhu, M., Fan, S., Wang, Z., Wu, X., Tang, J., et al. (2016). A Simple and Effective Ratiometric Fluorescent Probe for the Selective Detection of Cysteine and Homocysteine in Aqueous Media. *Molecules* 21 (8), 1023. doi:10.3390/molecules21081023

Qu, P., Ma, X., Chen, W., Zhu, D., Bai, H., Wei, X., et al. (2019). A Coumarin-Based Fluorescent Probe for Ratiometric Detection of Hydrazine and its Application in Living Cells. *Spectrochimica Acta Part A Mol. Biomol. Spectrosc.* 210, 381–386. doi:10.1016/j.saa.2018.11.007

Wang, K., Ye, Y.-X., Jiang, C.-Y., Guo, M.-Y., Zhang, X.-Y., Jiang, A.-Q., et al. (2021). Design and Synthesis of a Novel "Turn-On" Fluorescent Probe Based on Benzofuran-3(2h)-One for Detection of Hydrazine in Water Samples and Biological Systems. *Dyes Pigments* 194, 109587. doi:10.1016/j.dyepig.2021.109587

Wang, Y., Zhu, M., Jiang, E., Hua, R., Na, R., and Li, Q. X. (2017). A Simple and Rapid Turn on ESIPT Fluorescent Probe for Colorimetric and Ratiometric Detection of Biothiols in Living Cells. *Sci. Rep.* 7, 4377. doi:10.1038/s41598-017-03901-8

Xu, H., Huang, Z., Li, Y., Gu, B., Zhou, Z., Xie, R., et al. (2018a). A Highly Sensitive Naked-Eye Fluorescent Probe for Trace Hydrazine Based on 'C-CN' Bond Cleavage. *Analyst* 143 (18), 4354–4358. doi:10.1039/c8an01161c

Xu, W.-Z., Liu, W.-Y., Zhou, T.-T., Yang, Y.-T., and Li, W. (2018b). A Novel Fluorescein-Based "Turn-On" Probe for the Detection of Hydrazine and its Application in Living Cells. *Spectrochimica Acta Part A Mol. Biomol. Spectrosc.* 193, 324–329. doi:10.1016/j.saa.2017.12.040

Yan, F., Zhang, H., Li, X., Sun, X., Jiang, Y., and Cui, Y. (2021). A Fluorescein-Coumarin Based Ratiometric Fluorescent Probe for Detecting Hydrazine and its Real Applications in Cells Imaging. *Talanta* 223, 121779. doi:10.1016/j.talanta.2020.121779

Yan, S., Guo, H., Tan, J., Jiang, J., Liang, J., Yan, S., et al. (2020). Two Novel Spirobifluorene-Based Two-Photon Fluorescent Probes for the Detection of Hydrazine in Solution and Living Cells. *Talanta* 218, 121210. doi:10.1016/j.talanta.2020.121210

Yang, X., Liu, Y., Wu, Y., Ren, X., Zhang, D., and Ye, Y. (2017). A NIR Ratiometric Probe for Hydrazine "naked Eye" Detection and its Imaging in Living Cell. *Sensors Actuators B Chem.* 253, 488–494. doi:10.1016/j.snb.2017.06.165

Ye, H., Chen, L., Wang, X., and Lu, D. (2021). A Highly Sensitive Fluorescent Probe for Hydrazine Detection: Synthesis, Characterisation and Application in Living Cells. *Int. J. Environ. Anal. Chem.* 101 (8), 1086–1098. doi:10.1080/03067319.2019.1676422

Yin, B., Zhang, S., Chen, H., and Yan, L. (2021). A Cationic Organic Dye Based on Coumarin Fluorophore for the Detection of N2H4 in Water and Gas. *Sensors Actuators B Chem.* 344, 130225. doi:10.1016/j.snb.2021.130225

Zhang, S., Chen, D., Yan, L., Xie, Y., Mu, X., and Zhu, J. (2020a). A Near-Infrared Fluorescence Probe for Hydrazine Based on Dicyanoisophorone. *Microchem. J.* 157, 105066. doi:10.1016/j.microc.2020.105066

Zhang, S., Xie, Y., and Yan, L. (2020b). Ultra-fast and Visual Detection of Hydrazine Hydrate Based on a Simple Coumarin Derivative. *Spectrochimica Acta Part A Mol. Biomol. Spectrosc.* 230, 118028. doi:10.1016/j.saa.2020.118028

Zhang, T., Zhu, L., and Lin, W. (2021). A Near Infrared Ratiometric Fluorescent Probe with Aggregation Induced Emission (AIE) Characteristics for Hydrazine Detection *In Vitro* and *In Vivo*. *Dyes Pigments* 188, 109177. doi:10.1016/j.dyepig.2021.109177

Zhang, W., Huo, F., Liu, T., and Yin, C. (2018). Ratiometric Fluorescence Probe for Hydrazine Vapor Detection and Biological Imaging. *J. Mat. Chem. B* 6 (48), 8085–8089. doi:10.1039/c8tb02536c

Zhu, M., Ou, X., Tang, J., Shi, T., Ma, X., Wang, Y., et al. (2021a). Uptake, Distribution and Translocation of Imidacloprid-Loaded Fluorescence Double Hollow Shell Mesoporous Silica Nanoparticles and Metabolism of Imidacloprid in Pakchoi. *Sci. Total Environ.* 787, 147578. doi:10.1016/j.scitotenv.2021.147578

Zhu, M., Tang, J., Shi, T., Ma, X., Wang, Y., Wu, X., et al. (2022). Uptake, Translocation and Metabolism of Imidacloprid Loaded within Fluorescent Mesoporous Silica Nanoparticles in Tomato (Solanum lycopersicum). *Ecotoxicol. Environ. Saf.* 232, 113243. doi:10.1016/j.ecoenv.2022.113243

Zhu, M., Wu, X., Sang, L., Fan, F., Wang, L., Wu, X., et al. (2019). A Novel and Effective Benzo[d]thiazole-Based Fluorescent Probe with Dual Recognition Factors for Highly Sensitive and Selective Imaging of Cysteine *In Vitro* and *In Vivo*. *New J. Chem.* 43 (34), 13463–13470. doi:10.1039/c9nj03202a

Zhu, M., Xu, Y., Sang, L., Zhao, Z., Wang, L., Wu, X., et al. (2020). An ICT-Based Fluorescent Probe with a Large Stokes Shift for Measuring Hydrazine in Biological and Water Samples. *Environ. Pollut.* 256, 113427. doi:10.1016/j.envpol.2019.113427

Zhu, M., Zhao, Z., Huang, Y., Fan, F., Wang, F., Li, W., et al. (2021b). Hydrazine Exposure: A Near-Infrared ICT-Based Fluorescent Probe and its Application in Bioimaging and Sewage Analysis. *Sci. Total Environ.* 759, 143102. doi:10.1016/j.scitotenv.2020.143102

Conflict of Interest: The authors declare that the research was conducted in the absence of any commercial or financial relationships that could be construed as a potential conflict of interest.

Publisher's Note: All claims expressed in this article are solely those of the authors and do not necessarily represent those of their affiliated organizations, or those of the publisher, the editors and the reviewers. Any product that may be evaluated in this article, or claim that may be made by its manufacturer, is not guaranteed or endorsed by the publisher.